Rule-Based Control for a Flexible-Link Robot

Vivek G. Moudgal, Kevin M. Passino, *Member, IEEE*, and Stephen Yurkovich, *Senior Member, IEEE*

Abstract— **This paper presents a design and implementation case study that focuses on endpoint position control of a two degree-of-freedom robot with very flexible links. Linear and nonlinear conventional control techniques have been shown to be somewhat successful in achieving various control objectives for the laboratory test beds of this and many other studies; however, their reliance on an accurate mathematical model of the process often limits their chances of achieving good endpoint position control. Here we investigate an alternative to conventional approaches where we employ rule-based controllers to represent and implement two general forms of knowledge that we have about how to best control the mechanism: i) experience gained from the use of a mathematical model and conventional control; and ii) an intuitive understanding of the dynamics of the two-link flexible robot. We begin the case study by assuming that the controls for the two links of the robotic mechanism can be designed and implemented independently and investigate the performance of rule-based fuzzy controllers which only use simple intuitive knowledge about how to control two independent links. Next, we show that if the rule-base is augmented with knowledge about the coupling effects between the two links, the controller can achieve improved performance over the uncoupled case. The final portion of our case study, which represents our primary contribution, investigates the use of a two-level hierarchical rule-based controller with a simple upper-level "expert controller" that captures our knowledge about how to supervise the application of low-level fuzzy controllers during movements in the robot workspace. Overall, the rule-based supervisory control results have proven to be extremely effective for vibration suppression in the laboratory test bed of this study, comparing favorably (in terms of performance, design complexity, and implementation issues) to a variety of conventional techniques attempted to date (including linear robust designs, feedback linearization, input command shaping, and adaptive approaches).**

I. Introduction

FOR nearly a decade, control engineers and roboticists alike have been investigating the problem of controlling robotic mechanisms which have very flexible links. Such mechanisms are important in space structure applications, where large, lightweight robots are utilized in a variety of tasks, including deployment, spacecraft servicing, space station maintenance, etc. Flexibility is not designed into the mechanism; it is usually an undesirable characteristic which results from trading off mass and length requirements in optimizing effectiveness of the robot. These requirements and limitations of mass and rigidity give rise to many interesting issues from a control perspective. In this paper, we present a design case study which makes use of previous experience in modeling and control of a two-link planar flexible robot. Distinguishing features of the robotic mechanism and its operation are the use of structure-mounted sensing only (endpoint acceleration and joint position information) for feedback control, the focus on high speed, gross motion movements in endpoint positioning, and performance requirements for carrying significant payloads at the robot endpoint. Distinguishing features of the controller design primarily involve the use of a hierarchical structure and a rule-base for incorporating experience into the implementation.

Manuscript received September 25, 1993; revised June 6, 1994. Recommended by Associate Editor, K. Lorell. The work was supported in part by the National Science Foundation Grant IRI-9210332.

The authors are with the Department of Electrical Engineering, Ohio State University, Columbus, OH 43210-1272 USA.

IEEE Log Number 9406332.

A. Motivation for Rule-Based Control

The modeling complexity of multilink flexible robots is well documented, and numerous researchers have investigated a variety of techniques for representing flexible and rigid dynamics of such mechanisms. Equally numerous are the works addressing the control problem in simulation studies based on mathematical models under assumptions of perfect modeling. Even in simulation, however, a challenging control problem exists. It is well known that vibration suppression in slewing mechanical structures, whose parameters depend on the configuration (i.e., are time varying), can be extremely difficult to achieve. Compounding the problem, numerous experimental studies have shown that when implementation issues are taken into consideration, modeling uncertainties either render the simulation-based control designs useless or demand extensive tuning of controller parameters (often in an *ad hoc* manner). This is particularly true for mechanisms (such as laboratory test beds) built from low-cost components that do not age gracefully.

Hence, even if a relatively accurate model of the flexible robot can be developed, it is often too complex to use in controller development, especially for many control design procedures that require restrictive assumptions for the plant (e.g., linearity). It is for this reason that conventional controllers for flexible robots are developed either i) via simple crude models of the plant behavior that satisfy the necessary assumptions or ii) via the *ad hoc* tuning of simple linear controllers. Regardless, heuristics enter the design process when the conventional control design process is used.

It must be acknowledged, however, that such conventional control-engineering approaches that use appropriate heuristics to tune the design have been relatively successful. For a process such as a flexible robot, one is left with the following question: How much of the success can be attributed to the use of the mathematical model and conventional control design approach, and how much should be attributed to the clever heuristic tuning that the control engineer uses upon implementation? While control engineers have a relatively good understanding of the capabilities of conventional mathematical

approaches to control, much less is understood about whether or not control techniques that are designed to exploit the use of heuristic information (such as rule-based approaches) can perform better than conventional techniques.

B. Overview and Related Work

While most of the work to date for control of flexible-link robotic systems has used conventional control techniques, there has been recent interest in the literature in the use of intelligent control methodologies. In particular, the viewpoint expressed above, suggesting the need for control approaches which can incorporate operator knowledge for the process being controlled, is being recognized by more and more control engineers who apply control technologies. Since the literature abounds with work on the modeling and control of flexible robots, both from a theoretical (simulation-based) and experimental point of view, we refer the interested reader to [1, Chapter 8] for an overview of the literature on conventional approaches. Here, we focus primarily on recent work relevant to the case study of this paper and on previous work for the flexible-link robot under study.

One of the most promising techniques for flexible robot control used to date is that of input command shaping, where the system inputs (e.g., motor voltages) are "shaped" in such a manner that minimal energy is injected into the flexible modes of the system. So promising is this technology that a session at the 1993 American Control Conference [2] was devoted to the subject. Indeed, very good results using input-shaping with an outer-loop disturbance rejection controller for the two-link robot of this study were reported in [3]. Other works employing experimental verifications of input shaping schemes are appearing, such as [2], the ongoing study in [4] for controlling the endpoint movement of a large two-link robot, and the innovations of [5] for an adaptive implementation on a single-link apparatus. It is well known, however, that the primary difficulty of such command-shaping schemes lies in the fact that they are open-loop strategies and require relatively precise knowledge of the system dynamics. Any attempt to improve robustness to uncertainties (such as placing the shaper in the loop or increasing the filter order) result in delays in the system response, which may or may not be tolerable.

It should be mentioned that recent work in the area of two-time scale (singular perturbation) approaches for vibration suppression in flexible mechanical structures show promise. The control objective in those investigations is different than that of the present study, since in the former the primary focus is on disturbance rejection effects (small deflections) after larger slew motions are complete; also inherent in these techniques is the need for accurate models of the system dynamics. Some experimental work utilizing embedded piezoelectrics and piezoceramics has begun to appear. Other recent conventional approaches to the problem of flexible robot control include the work in [6] for the use of linear (state feedback) techniques where a fast state estimator is employed in small-angle movements and in [7] where gross-motion movements for a single flexible link are studied in the case of adaptation for payload tasks. As for previous work in developing conventional controllers for flexible robotic test beds at Ohio State (including the two-link apparatus of the current study), the control developed in [8] used a nonlinear inversion (feedback linearization) control law for rigid dynamics, with separate loops for flexure effects. The study in [9] investigated and compared time-domain and frequency-domain identification techniques on a single-link robot, and the work in [10], [11] developed time- and frequency-domain identification and control schemes for payload adaptation, which were later employed on a two-link apparatus [12].

As noted above, the literature has recently seen an emergence of results using intelligent control technologies. Fuzzy logic, neural networks, and hierarchical schemes have been investigated for flexible robotic mechanisms. For example, a recent paper [13] uses fuzzy logic for a fast-moving single-link apparatus, focusing on smooth, rigid body motion control. In [14], a fuzzy learning control approach is used for the same laboratory test bed as the current study. The focus there, however, was on automatic synthesis of a direct fuzzy controller and its subsequent tuning when there are payload variations. In [15], [16] a fuzzy logic supervisory level is used for lower-level conventional controller selection and tuning for the same laboratory test bed as is used in the current study. Motivated by the success of those studies, the control scheme of this paper builds on the idea of supervising lower level controllers in a hierarchy and improves on all previous results by using rule-based controllers at the lower level (this paper is an expanded version of the work reported in [17]).

In Section II, we provide a detailed description of the two-link flexible robot used in this study and then describe a case-study approach to the design of a rule-based control scheme. In Section III, we investigate the implementation of two types of direct fuzzy controllers. In the first type, we employ simple intuitive knowledge, which views the robot as two separate links, in construction of the fuzzy controller rule-base. Experiments for various slews and payload conditions are reported to verify the effectiveness of the "uncoupled" direct fuzzy controller. Next, we show that if extra information about the coupling effects of the two links (e.g., that the acceleration of the shoulder link will affect the acceleration in the elbow link) is loaded into the rule-base, then significant improvements can be realized. Although there has been much recent interest in the use of fuzzy control in robotics and in particular for flexible robots, this is, to our knowledge, the first application of fuzzy control to a two-link flexible robot where endpoint acceleration is used as a feedback variable.

In Section IV it is shown how a simple rule-based "expert controller" [18], [19] can be used in the upper level of a two-layer hierarchical rule-based controller to supervise a direct fuzzy controller at a lower level. Such a rule-based supervisory controller implements our knowledge about how to choose the best direct fuzzy controller to apply during a slew (we have actually gained the insight into how to choose the controller via our past experience in developing and implementing conventional controllers for this robot). Hence, a rule-based supervisor provides for the incorporation of additional information about how to achieve better slew rates and vibration damping; experimental results for various

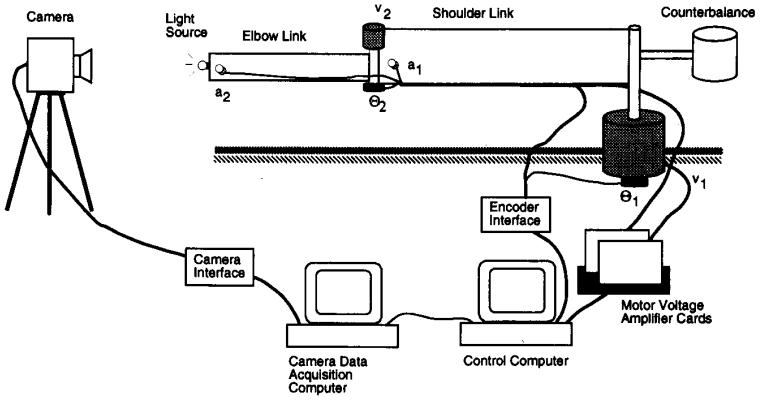

Fig. 1. Two-link flexible robot setup.

slews and payload conditions are presented. It is important to note that while our rule-based supervisory control approach is novel, there have been several previous related investigations on rule-based supervisory control. In addition to [15], [16], the authors in [20]–[23] study fuzzy supervisory controllers that tune conventional controllers, especially ones that tune PID controllers. We emphasize that while there are some relationships between supervisory and conventional and fuzzy adaptive control (e.g., the fact that in both supervisory and adaptive control the underlying controller is being tuned) the mechanisms for tuning are significantly different [14]–[16], [24]–[26].

II. Laboratory Test Bed

The two-link flexible robot shown in Fig. 1 consists of three principle parts: the robot with its sensors, the computer and the interface to the robot, and the camera with its computer and interface. The robot is made up of two very flexible links constrained to operate in the horizontal plane. The "shoulder link" is a counter-balanced aluminum strip 75 cm long, 12.7 cm tall, and 0.23 cm thick and is driven by a dc direct drive motor with a stall torque of 4.802 N-m. The "elbow link," mounted on the shoulder link endpoint, is an aluminum strip 50 cm long, 3.8 cm tall, and 0.1 cm thick. The actuator for the elbow link is a 28 volt dc, geared motor (30:1) with a stall torque of 2.53×10^{-3} N-m. The sensors on the robot are two optical encoders for the motor shaft positions Θ_1 and Θ_2 and two accelerometers mounted on the link endpoints to measure the accelerations a_1 and a_2.

Extensive identification and modeling exercises have resulted in reliable models for the motor/amplifier configurations for this mechanism. The shoulder-motor amplifier is a voltage-to-current (transconductance) amplifier, whereas the elbow-motor amplifier is voltage-to-voltage. Because both amplifiers close a velocity loop with their respective motor, we chose to develop combined motor-amplifier models (through empirical identification exercises) for analysis. These models enable simulation and control design studies for rigid dynamics. In that case, because no torque sensors are employed for this apparatus, dynamics were derived relating the amplifier-motor input voltages to the robot joint input torques. Thus, control input laws are expressed in terms of voltages (v_1 and v_2, voltages at the motor terminals) rather than torques.

A Reticon LC-310 line scan camera interfaced to an IBM PC XT is used to monitor the endpoint position of the robot for plotting; this data is not used for feedback. For comparative purposes in this paper, we use the camera data for robot movements which end in a fully-extended position and which begin in some position to approximate equal movements in each joint. When responses are plotted, the final endpoint position is nominally indicated (on the plot) to reflect (approximately) the total movement, in degrees, of the shoulder joint. Because movements are constrained to the horizontal plane, there are no gravity effects on the motors, and therefore it is appropriate to express performance (setpoints) in terms of joint angles. We note that constraining the robot to operate in the horizontal plane is done precisely for these reasons (to remove gravity effects), since the primary application for this work is large, lightweight robots in space.

The control computer for the robot is a PC with an Intel 80386SX operating at 25 megahertz. The computer interface hardware used by the control computer is a Keithley MetraByte DAS1600 and a Scientific Solutions Lab Tender card. The camera computer uses a Scientific Solutions Lab Tender card. The camera interface and the encoder interface are additional circuits designed and built in house [27] for signal conditioning.

The primary objective of this research is to develop a controller that makes the robot move to its desired position as quickly as possible with little or no endpoint oscillation. To appreciate the improvement in the plant behavior due to the application of the various control strategies, we will first look at how the robot operates under the no-control situation, that is, when no external digital control algorithm is applied for vibration compensation. To implement the no-control case we simply apply $v_1 = v_2 = 0.3615$ volts at $t = 0$ seconds and return v_1 and v_2 to zero voltages as soon as the links reach their setpoints. Note that for this experiment, we monitor the movement of the links but do not use this information as feedback for control.

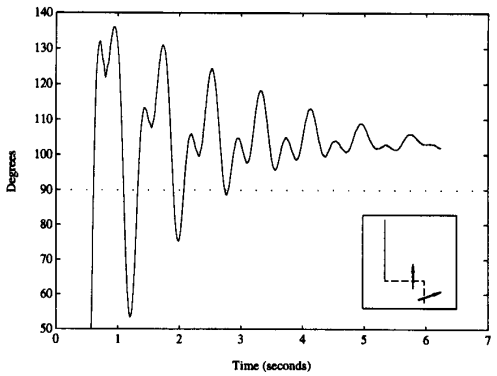

Fig. 2. Endpoint position: No-control response.

The result of the no-control experiment is given in Fig. 2 where the endpoint position shows a significant amount of endpoint oscillation. As is typical in mechanisms of this sort, inherent modal damping is present; for our robot, the damping ratios associated with the dominant modal frequencies, 2.5 Hz and 1.2 Hz, are 0.65 and 0.11, respectively (determined empirically). It is well known that the effect of mass-loading a slewing flexible beam is to reduce the modal frequencies. Indeed, when a 30–gram payload is attached to the robot endpoint, the first modal frequency of the second link (endpoint) reduces to less than 2 Hz. This effect causes performance degradation in fixed, linear controllers [5], [9], [10]. In Fig. 2, as in all plots to follow, endpoint position refers to the position of the elbow link endpoint. Note that the inset shown in Fig. 2 depicts the robot slew employed. The two dashed lines describe the initial position of the links. The arrows show the direction of movement, and the solid line shows the final position of the links. Hence, for this open-loop experiment we wanted 90 degrees of movement in each link. In the ideal case, the shaft should stop moving the instant the voltage signal to the motor amplifier is cut off. But the arm had been moving at a constant velocity before the signal was cut off, and thus has a momentum which will drag the shaft past the angle at which it was to stop. This movement depends on the speed at which the arm was moving which, in turn, depends on the voltage signal applied. Clearly, there is a significant need for vibration damping in endpoint positioning. Quantitatively speaking, in terms of step-type responses (for motions through large angles in each joint), the control objectives are as follows: system settling (elimination of residual vibrations in endpoint position) within two seconds of motion initiation, and overshoot minimized to be less than 5% deviation from final desired position. In addition, we wish to achieve certain qualitative aspects such as elimination of jerk and smoothness in transition between commanded motions.

III. Direct Fuzzy Control

In this section, we investigate the use of two types of direct fuzzy controllers for the flexible robot: one that uses information about the coupling effects of the two links (coupled direct fuzzy control) and one which does not use such information (uncoupled direct fuzzy control). The design scenario we present, although specific to the flexible robot testbed under study, may be viewed as following a general philosophy for fuzzy controller design. Throughout, it is assumed that the reader has knowledge of basic concepts in the area of fuzzy control.

A. Uncoupled Direct Fuzzy Control

For uncoupled direct fuzzy control, two separate controllers are implemented, one for each of the two links. Each controller has two inputs and one output as shown in Fig. 3. The term "uncoupled" is used, since the controllers operate independent of each other. No information is transferred from the shoulder-motor controller to the elbow-motor controller or back. We thus consider the robot to be made up of two separate single link systems. In Fig. 3, Θ_{1d} and Θ_{2d} denote the desired positions of the shoulder and the elbow links, respectively, and $\Theta_1(t)$ and $\Theta_2(t)$ denote their position at time t, as measured from the optical encoders. The inputs to the shoulder link controller are the position error of the shoulder-motor shaft $e_1(t) = \Theta_{1d} - \Theta_1(t)$ and the acceleration information $a_1(t)$ from the shoulder link endpoint. The output of this controller is multiplied by the output gain g_{v1} to generate the voltage signal $v_1(t)$ that drives the shoulder-motor amplifier. The inputs to the elbow link controller are the elbow-motor shaft position error $e_2(t) = \Theta_{2d} - \Theta_2(t)$ and the acceleration information from the elbow link endpoint $a_2(t)$. The output of this controller is multiplied by the output gain g_{v2} to generate the voltage signal $v_2(t)$ that drives the elbow-motor amplifier.[1]

The input and the output universes of discourse of the fuzzy controller are normalized on the range [-1, 1]. The gains g_{e1}, g_{e2}, g_{a1}, and g_{a2} are used to map the actual inputs of the fuzzy system to the normalized universe of discourse [-1, 1] and are called "normalizing gains." Similarly g_{v1} and g_{v2} are the output gains to scale the output of the controllers. We use singleton fuzzification and center of gravity (COG) defuzzification throughout this paper and the min operator for the premise and implication [28].

1) Rule-Base: The shoulder controller uses triangular membership functions as shown in Fig. 4. Notice that the membership functions for the input fuzzy sets are uniform, but the membership functions for the output fuzzy sets are narrower near zero. Experience has shown that this serves to increase the gain of the controller near the setpoint so we can obtain a better steady-state control and yet avoid excessive overshoot. The membership functions for the elbow controller are similar, but they have different center values for the membership functions as they use different universes of discourse than the shoulder controller. For the shoulder controller, the universe of discourse for the position error is chosen to be [-250,

[1] We experimented with using the change in position error of each link as an input to each of the link controllers, but found that it significantly increased the complexity of the controllers with very little, if any, improvement in overall performance; hence, we did not purse the use of this controller input. Typically, we use filtered signals from the accelerometers, prior to processing, to enhance their effectiveness.

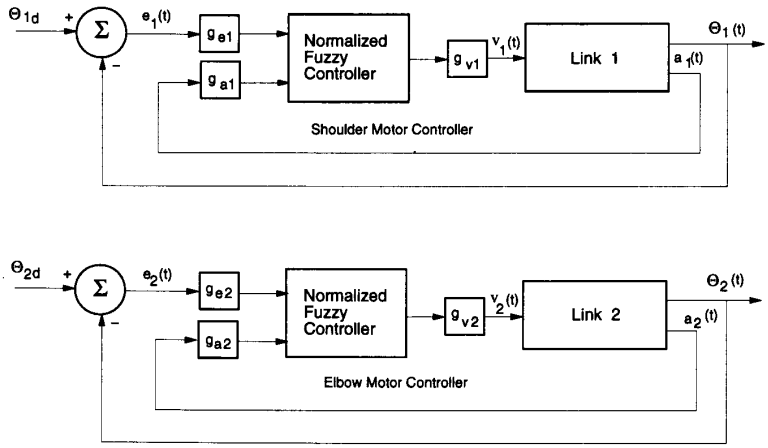

Fig. 3. Fuzzy control system for uncoupled controller.

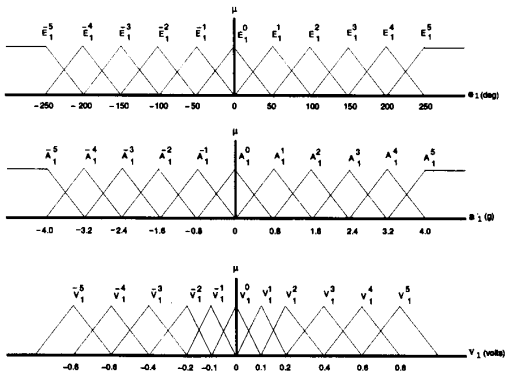

Fig. 4. Membership functions for the shoulder controller.

+250] degrees.[2] The universe of discourse for the endpoint acceleration of the shoulder link is [-4, +4] g. This width of 8g was picked after experimentation with different slews at different speeds, upon observing the output of the acceleration sensor. The output universe of discourse of [-0.8, +0.8] volts was chosen so as to keep the shaft speed within reasonable limits.

For the elbow-motor controller, the universe of discourse for the error input is [-250, +250] degrees. This motor is mounted on the shoulder-link endpoint, and the link movement is limited by the shoulder link. The universe of discourse for the acceleration input is [-8, +8] g which was picked after several experiments. The universe of discourse for the output of the elbow controller is [-5, +5] volts. This universe of discourse is large compared to the shoulder link as this motor is a geared head motor with a 30:1 reduction in the motor to the output shaft speed.

The rule-base array that we use for the shoulder controller is shown in Fig. 5, and for the elbow link it is shown in Fig. 6. Each rule-base is an 11×11 array, as we have 11 fuzzy sets on the input universes of discourse. The topmost row shows the indexes for the 11 fuzzy sets for the acceleration input a_1 and the column at extreme left shows the indexes for the 11 fuzzy sets for the position error input e_1. The body of the array shows the indexes m for V_1^m in fuzzy implications of the form

$$\text{If } E_1^j \text{ and } A_1^k \text{ Then } V_1^m$$

where E_i^j, A_i^j, and V_i^j; $(i = 1, 2; -5 \leq j \leq +5)$ denote the jth fuzzy sets associated with e_i, a_i, v_i, respectively. Notice the uniformity of the indexes in Figs. 5 and 6 and that for row $j = 0$ there are three zeros in the center. These zeros have been placed so as to reduce the sensitivity of the controller to the noise output from the accelerometer. These zeros do not make the controller have zero gain for all small values of the acceleration signal. Via the interpolation performed by the fuzzy controller, these zeros simply lower the gain near zero to make the controller less sensitive so that it will not amplify disturbances. The number of rules used for the uncoupled direct fuzzy controller is 121 for shoulder controller, plus 121 for elbow controller, giving a total of 242 rules.

2) Results: The plant output response and the two controller outputs of the uncoupled fuzzy system are shown in Fig. 7. Fig. 7(a) shows the endpoint position response for this controller design. The robot was commanded to slew 90 degrees for each link from the initial position shown by the dashed lines in the inset to its fully-extended position shown by the solid lines.[3] From the plot, it is seen that the magnitude of the endpoint oscillations is reduced as compared to the no-control case, and the settling time is also improved (see Fig. 2). In the

[2]Note that in this paper, we will refer to $[X, Y]$ as being the universe of discourse while in actuality the universe of discourse is made up of all reals (e.g., in Fig. 4 we will refer to the universe of discourse of $e_1(t)$ as [-250, +250]). In addition, will refer to $Y - X$ as being the "width" of the universe of discourse (so that the width of the universe of discourse [-250, +250] is 500). Moreover, note that by specifying the width for the universes of discourse, we are also specifying the corresponding scale factor. For example, if the input universe of discourse for $e_1(t)$ is [-250, +250], then $g_{e1} = \frac{1}{250}$, and if the output universe of discourse for $v_1(t)$ is [-0.8, +0.8] the $g_{v1} = 0.8$.

[3]Although typical experiments investigate movements for the entire workspace, the fully extended final position is utilized throughout for convenience, due primarily to the camera's effective geometry. Moreover, out-of-plane movements, which are not addressed in this study (see, [16]), are minimized in this configuration.

V_1^n / E_1^j	A_1^k										
	-5	-4	-3	-2	-1	0	+1	+2	+3	+4	+5
-5	-5	-5	-5	-4	-4	-3	-3	-2	-2	-1	0
-4	-5	-5	-4	-4	-3	-3	-2	-2	-1	0	+1
-3	-5	-4	-4	-3	-3	-2	-2	-1	0	+1	+2
-2	-4	-4	-3	-3	-2	-2	-1	0	+1	+2	+2
-1	-4	-3	-3	-2	-2	-1	0	+1	+2	+2	+3
0	-4	-3	-2	-1	0	0	0	+1	+2	+3	+4
+1	-3	-2	-2	-1	0	+1	+2	+2	+3	+3	+4
+2	-2	-2	-1	0	+1	+2	+2	+3	+3	+4	+4
+3	-2	-1	0	+1	+2	+2	+3	+3	+4	+4	+5
+4	-1	0	+1	+2	+2	+3	+3	+4	+4	+5	+5
+5	0	+1	+2	+2	+3	+3	+4	+4	+5	+5	+5

Fig. 5. Rule-base for shoulder link.

V_2^n / E_2^j	A_2^k										
	-5	-4	-3	-2	-1	0	+1	+2	+3	+4	+5
-5	-5	-5	-4	-4	-3	-3	-3	-2	-2	-1	0
-4	-5	-4	-4	-3	-3	-3	-2	-2	-1	0	+1
-3	-4	-4	-3	-3	-3	-2	-2	-1	0	+1	+2
-2	-4	-3	-3	-3	-2	-2	-1	0	+1	+2	+2
-1	-4	-3	-3	-2	-2	-1	0	+1	+2	+2	+3
0	-4	-3	-2	-1	0	0	0	+1	+2	+3	+4
+1	-3	-2	-2	-1	0	+1	+2	+2	+3	+3	+4
+2	-2	-2	-1	0	+1	+2	+2	+3	+3	+3	+4
+3	-2	-1	0	+1	+2	+2	+3	+3	+3	+4	+4
+4	-1	0	+1	+2	+2	+3	+3	+3	+4	+4	+5
+5	0	+1	+2	+2	+3	+3	+3	+4	+4	+5	+5

Fig. 6. Rule-base for elbow link.

initial portion of the response (between 0.8 and 2.0 sec.) we see large oscillations, due to the fact that the controllers are uncoupled. That is, the shoulder link comes close to its setpoint at around 0.9 seconds, but is still traveling at a high speed. When the controller detects this, it tries to cut the speed of the link by applying an opposite voltage seen by the negative spike in Fig. 7(b) at around 0.9 seconds. This causes the endpoint of the elbow link to accelerate due to its inertia, causing it to oscillate with a larger magnitude. When the controller for the elbow link detects this sudden change in the condition it outputs a large signal to move the shaft in the direction of acceleration so as to damp these oscillations; this can be seen in the controller output plot for the elbow-motor in Fig. 7(c). Once the oscillations are damped out, the controller continues to output signals until the setpoint is reached.

Note that a portion of the oscillation is caused by the dead zone nonlinearity in the gearbox of the elbow-motor. The sudden braking of the shoulder link causes the elbow link to jerk and the link oscillates in the dead zone, creating what is similar to a limit cycle effect. One way of preventing these oscillations in the link is to slow down the speed of the elbow link until the shoulder link is moving fast and speed it up as the shoulder link slows down. This would ensure that the elbow link is not allowed to oscillate as the motor is moving fast and the driven gear does not operate in the dead zone. This control technique will be examined in the next section when we couple the acceleration feedback signals from the robot.

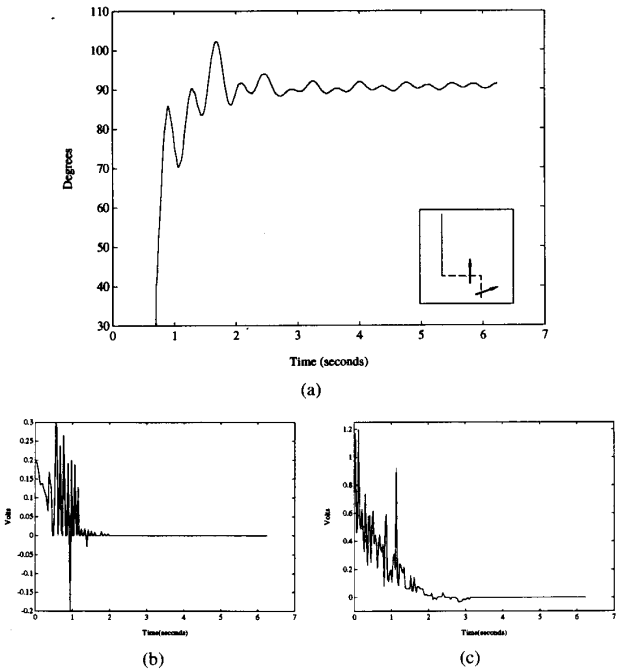

Fig. 7. (a) Endpoint position for uncoupled controller design, (b) Shoulder link input voltage v_1, (c) Elbow link input voltage v_2.

Fig. 8 shows the robot response for a "counter-relative" movement (links moving in opposite directions). The requested slew is 90 degrees for each link and is shown in the inset. Notice that we get a similar response to that found in Fig. 7; the hump seen in the plot at about one second is due to the geometry of the commanded slew. As seen from the inset, the shoulder link is commanded to move clockwise and the elbow link is commanded to move counterclockwise. The camera is placed so that when both the links have completed their slews, the tip of the elbow link endpoint is pointed directly at the camera. The shoulder link moves so as to bring the endpoint into the visual range of the camera, but at the same time the elbow link is moving in the opposite direction. If the speed of the elbow link is greater than the speed of the shoulder link, at that point it appears as a hump in the data collected by the camera.

Although our primary focus in this study is on gross motion control (for large angle movements), it is important to investigate performance for smaller movements as well. Fig. 9 shows the robot response to a small slew of 20 degrees for each link. As expected, we obtain improved performance results as compared to the large angle slews shown in Figs. 7 and 8. Notice that the slew is completely in the visual region of the camera, yet we do not see a total movement of 40 degrees. This is because even though each link moves 20 degrees, the arc traveled by the light source at the elbow link endpoint is less than 40 degrees (this can be seen by considering the geometry of the hardware setup).

Fig. 10 shows the response of the plant with a payload. The payload used was a 30–gram block of aluminum attached to

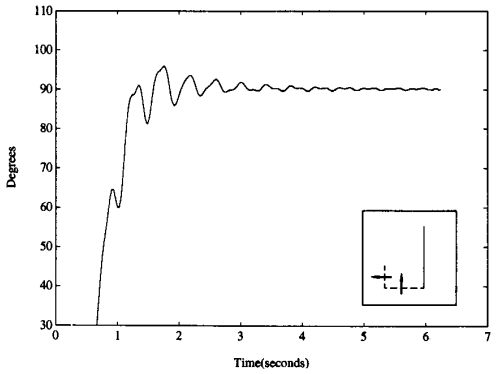

Fig. 8. Endpoint position for counter-relative slew for uncoupled control.

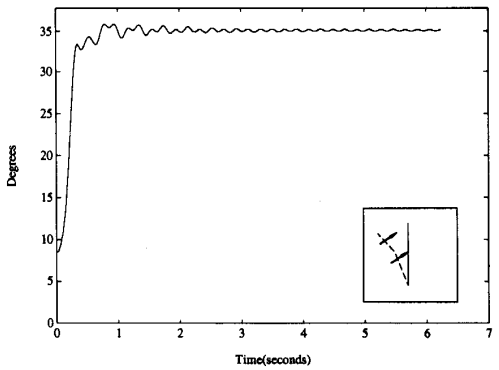

Fig. 9. Endpoint position for small slews using uncoupled control.

the elbow link endpoint. A slew of 90 degrees for each link was commanded as shown in the inset. The payload at the end of the elbow link increases the inertia of the link and reduces the modal frequencies of oscillation. In this case, this reduction in the frequency positively affected the controller's ability to dampen the oscillation caused due to the dead zone as compared to the unloaded case shown in Fig. 7.

B. Coupled Direct Fuzzy Control

While the two uncoupled controllers provide reasonably good results, they are not able to take control actions that are directly based on the movements in both links. In this section we investigate the possibility of improving the performance by coupling the two controllers. This can be done by using either the position information, the acceleration information, or both. From the tests on the independent controllers, it was observed that the acceleration at the endpoint of the shoulder link significantly affected the oscillations of the elbow link endpoint, whereas the acceleration at the endpoint of the elbow link did not significantly affect the shoulder link. The position of one link does not have a significant effect on the vibrations in the other link. As the primary objective here is to reduce the vibration at the endpoint as much as possible while still achieving adequate slew rates, it was decided to couple the controller for the elbow link to the shoulder link using the acceleration feedback from the endpoint of the shoulder link;

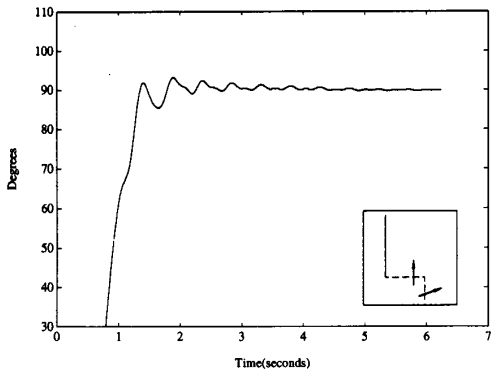

Fig. 10. Endpoint position for uncoupled controller design with payload.

this is shown schematically in Fig. 11. Note that in addition to the six normalizing gains g_{e1}, g_{e2}, g_{a1}, g_{a2}, g_{v1}, and g_{v2}, a seventh gain g_{a12} is added to the system. This gain can also be varied to tune the controller and need not be the same as g_{a1}.

1) Rule-Base: The rule-base and the membership functions for the shoulder link are kept the same as in Figs. 4 and 5, and the rule-base for the elbow link is modified to include the acceleration information from the shoulder link endpoint. Adding a third left-hand side element to the premises of the rules in the rule-base in this manner will, of course, increase the total number of rules. The number of fuzzy sets for the elbow controller was therefore reduced to seven to keep the number of rules at a reasonable level. The number of rules for the second link with seven fuzzy sets increased to 343 ($7 \times 7 \times 7$). Hence, the number of rules used for the coupled direct fuzzy controller is 121 for shoulder controller, plus 343 for elbow link controller, for a total of 464 rules. The membership functions for the elbow controller are shown in Fig. 12. The universe of discourse for the position error is [-250, +250] degrees, and for the elbow link endpoint acceleration it is [-8, +8] g as in the uncoupled case. The universe of discourse for the shoulder link acceleration is [+2, -2] g. This smaller range was chosen to make the elbow link controller sensitive to small changes in the shoulder link endpoint oscillation. The universe of discourse for the output voltage is [-4, +4] volts. Fig. 13(a)–(g) depicts a three dimensional rule-base. Fig. 13(d) represents the case when the acceleration input from the shoulder link is zero and is the center of the rule-base (the body of the table denotes the indexes m for V_2^m). Fig. 13(a)–(c) are for the case when the shoulder endpoint acceleration is negative, and Fig. 13(e)–(g) are for the case where the shoulder endpoint acceleration is positive. The central portion of the rule-base makes use of the entire output universe of discourse. This is the portion of the rule-base where the acceleration input from the shoulder link endpoint is zero or small. As we move away from the center of the rule base (to the region where the shoulder link endpoint acceleration is large), only a small portion of the output universe of discourse is used to keep the output of the controller small. Thus, the speed of the elbow link is dependent on the acceleration input from the shoulder link endpoint. The speed of the elbow link is decreased if the acceleration is large and is increased as

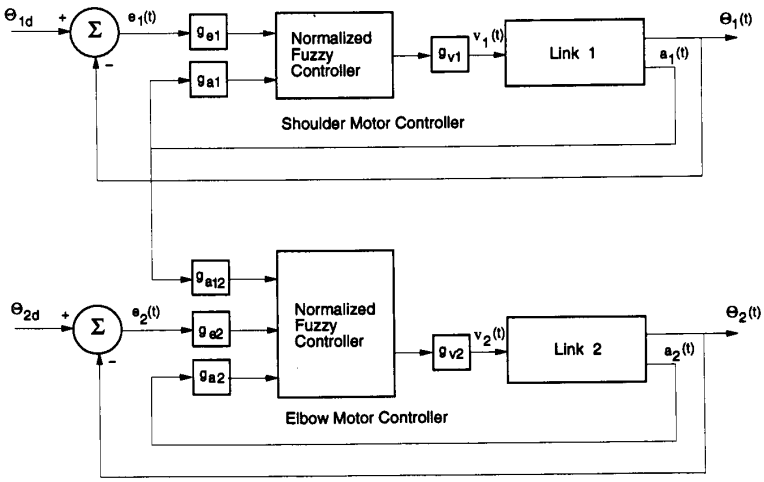

Fig. 11. Fuzzy control system design for direct fuzzy controller design.

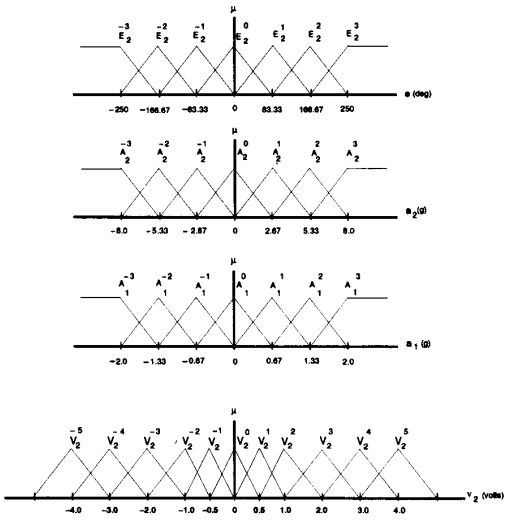

Fig. 12. Membership functions for the elbow controller using coupled control.

the acceleration input decreases. Also note in Fig. 13(c)–(e) that there are three zeros in the middle rows to reduce the sensitivity of the controller to the noisy accelerometer signal. This noise is not a significant problem when the endpoint is oscillating, and so the rule-base does not have the zeros in the outer region. Taking the rule-base as a three-dimensional array we get a central cubical core made up of zeros. Also notice that some parts of the rule-base, especially towards the extremes of the third dimension, are not fully uniform. This has been done to slow down the elbow link when the acceleration input from the shoulder link is very large.

The coupled direct fuzzy controller seeks to vary the speed of the elbow link depending on the amplitude of oscillations in the shoulder link. If the shoulder link is oscillating too much, the speed of the elbow link is reduced so as to allow the oscillations in the shoulder link to be damped, and if there are no oscillations in the shoulder link then the second link speed is increased. We do this to eliminate the oscillation of the elbow link close to the setpoint where the control voltage from the elbow controller is small. This scheme works well as will be shown by the results, but the drawback is that it slows down the overall plant response as compared to the uncoupled case (i.e., it slows the slew rate).

2) Results: The experimental results obtained using coupled direct fuzzy control are shown in Fig. 14. The slew requested here is the same as in the case of the uncoupled direct fuzzy control experiment (Fig. 7) as shown by the inset (90 degrees for each link). Note that there is no overshoot in the response, with negligible residual vibrations. The dip in the curve in the initial part of the graph is due to the first link "braking" as it reaches the setpoint, primarily because of the dead zone nonlinearity in the gears. As the shoulder link brakes, the elbow link is accelerated due to its inertia. The elbow link, which was at one end of its dead zone while the shoulder was moving, shoots to the other end of the dead zone causing the local maxima seen in Fig. 14(a) at around 0.9 seconds. The link recoils due to its flexibility and starts moving to the lower end of the dead zone. By this time the elbow-motor speed increases and prevents further oscillation of the elbow link in the dead zone. Notice that the multiple oscillations in the elbow link have been eliminated as compared to Fig. 7. This is due to the fact that when the shoulder link reaches its setpoint the elbow link is still away from its setpoint and, as the shoulder link slows down, the elbow link motor speeds up and keeps the elbow link at one end of the dead zone preventing oscillation. Also notice that the rise time has increased in this case, compared to that of the uncoupled case due to the decrease in speed of the second link while the first link is moving. This fact (increase in rise time) and, especially, the schema embodied in the coupled-controller rule-base contribute to the reduction in endpoint residual vibration. Experimentally, we have determined that

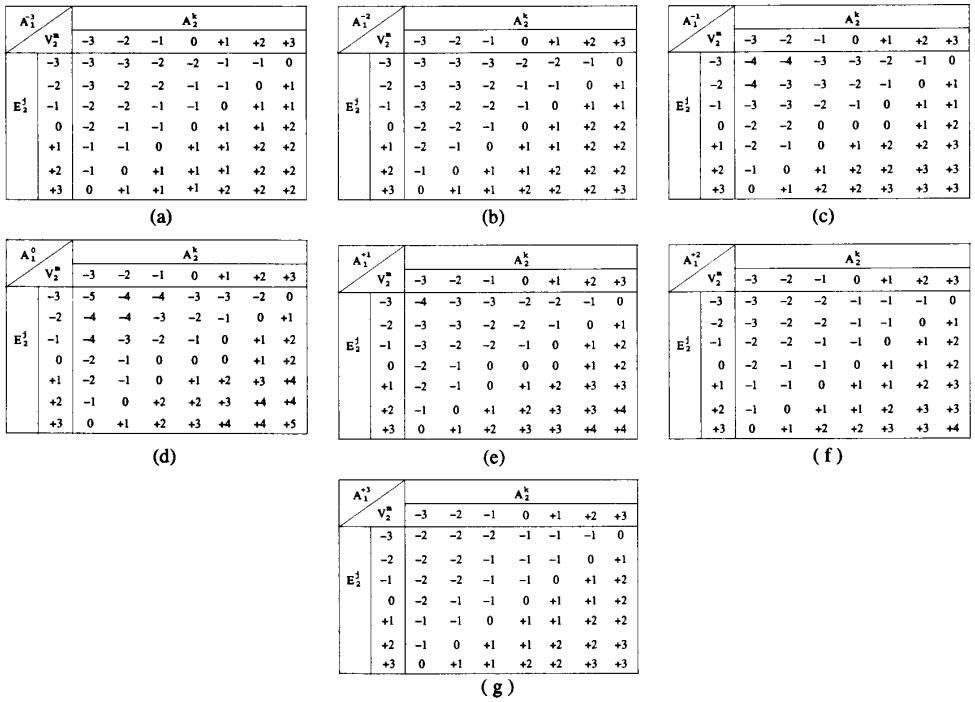

(a)

A_1^3 / V_2^m	A_2^k −3	−2	−1	0	+1	+2	+3
−3	−3	−3	−2	−2	−1	−1	0
−2	−3	−2	−2	−1	−1	0	+1
E_2^j −1	−2	−2	−1	−1	0	+1	+1
0	−2	−1	−1	0	+1	+1	+2
+1	−1	−1	0	+1	+1	+2	+2
+2	−1	0	+1	+1	+1	+2	+2
+3	0	+1	+1	+1	+2	+2	+2

(b)

A_1^{-2} / V_2^m	A_2^k −3	−2	−1	0	+1	+2	+3
−3	−3	−3	−3	−2	−2	−1	0
−2	−3	−3	−2	−1	−1	0	+1
E_2^j −1	−3	−2	−2	−1	0	+1	+1
0	−2	−2	−1	0	+1	+2	+2
+1	−2	−1	0	+1	+1	+2	+2
+2	−1	0	+1	+1	+2	+2	+2
+3	0	+1	+1	+2	+2	+2	+3

(c)

A_1^{-1} / V_2^m	A_2^k −3	−2	−1	0	+1	+2	+3
−3	−4	−4	−3	−3	−2	−1	0
−2	−4	−3	−3	−2	−1	0	+1
E_2^j −1	−3	−3	−2	−1	0	+1	+1
0	−2	−2	0	0	0	+1	+2
+1	−2	−1	0	+1	+2	+2	+3
+2	−1	0	+1	+2	+2	+3	+3
+3	0	+1	+2	+2	+3	+3	+3

(d)

A_1^0 / V_2^m	A_2^k −3	−2	−1	0	+1	+2	+3
−3	−5	−4	−4	−3	−3	−2	0
−2	−4	−4	−3	−2	−1	0	+1
E_2^j −1	−4	−3	−2	−1	0	+1	+2
0	−2	−1	0	0	0	+1	+2
+1	−2	−1	0	+1	+2	+3	+4
+2	−1	0	+2	+2	+3	+4	+4
+3	0	+1	+2	+3	+4	+4	+5

(e)

A_1^{+1} / V_2^m	A_2^k −3	−2	−1	0	+1	+2	+3
−3	−4	−3	−3	−2	−2	−1	0
−2	−3	−3	−2	−2	−1	0	+1
E_2^j −1	−3	−2	−2	−1	0	+1	+2
0	−2	−1	0	0	0	+1	+2
+1	−2	−1	0	+1	+2	+3	+3
+2	−1	0	+1	+2	+3	+3	+4
+3	0	+1	+2	+3	+3	+4	+4

(f)

A_1^{+2} / V_2^m	A_2^k −3	−2	−1	0	+1	+2	+3
−3	−3	−2	−2	−1	−1	−1	0
−2	−3	−2	−2	−1	−1	0	+1
E_2^j −1	−2	−2	−1	−1	0	+1	+2
0	−2	−1	−1	0	+1	+1	+2
+1	−1	−1	0	+1	+1	+2	+3
+2	−1	0	+1	+1	+2	+3	+3
+3	0	+1	+2	+2	+3	+3	+4

(g)

A_1^{+3} / V_2^m	A_2^k −3	−2	−1	0	+1	+2	+3
−3	−2	−2	−2	−1	−1	−1	0
−2	−2	−2	−1	−1	−1	0	+1
E_2^j −1	−2	−2	−1	−1	0	+1	+2
0	−2	−1	−1	0	+1	+1	+2
+1	−1	−1	0	+1	+1	+2	+2
+2	−1	0	+1	+1	+2	+2	+3
+3	0	+1	+1	+2	+2	+3	+3

Fig. 13. Rule-base array for the elbow link.

the dip in the curve can be decreased, but not completely eliminated as the rule-base does not have enough "granularity" near zero. To alleviate this problem, a "supervisor" can be used to change the granularity of the rule-base as the shoulder link comes close to its desired point by changing the universes of discourse and the appropriate normalizing gains. This would produce finer control close to the setpoint resulting in a smoother transition in the speed of the shoulder link. We will investigate the use of such a supervisor in the next section.

Fig. 15 shows the response of the robot to counter-relative slews. The requested slews were the same as in the uncoupled case (90 degrees for each link) shown in Fig. 8. The response shows a marked improvement in the settling time and the amplitude of the oscillations compared to the uncoupled case (Fig. 8). The initial hump seen in the plot at 0.5 seconds is due to the nature of the commanded slew as explained in Section III (A-2).

Fig. 16 shows the response of the robot to a small slew. The commanded slew is 20 degrees for both the links and is shown in the inset. The plot shows an improvement in the settling time and the amplitude of the oscillations as compared to the uncoupled case (Fig. 9).

Fig. 17 shows the endpoint response of the robot with a 30–gram payload attached to its endpoint. The commanded slew is 90 degrees for each link as shown in the inset. Notice that the dip in the curve (between 1.0 to 1.5 sec) is reduced as compared to the case without payload (Fig. 17). This is due to the increased inertia of the elbow link, which reduces the frequency of oscillation of the link, as the elbow link motor speeds up at this point preventing further oscillations.

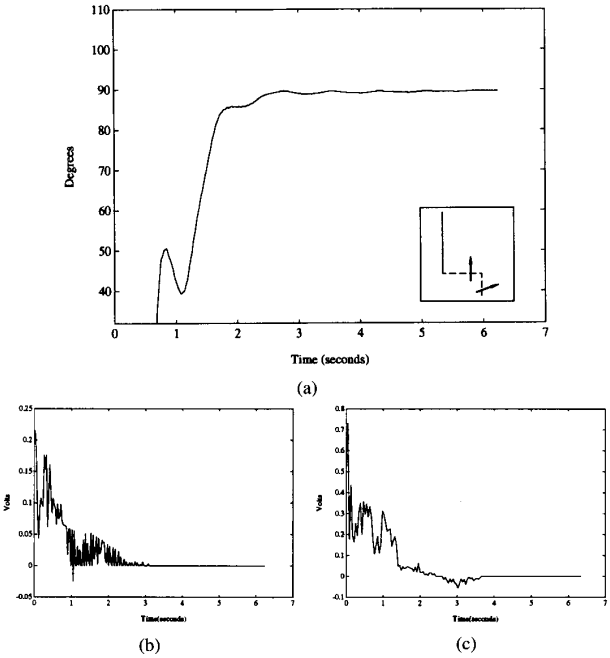

(a) (b) (c)

Fig. 14. (a) Endpoint position for coupled controller design, (b) Shoulder link input voltage v_1, (c) Elbow link input voltage v_2.

Obviously, there is performance degradation due to the fact that the modal frequencies of the flexible links (particularly the elbow link) have changed with the additional payload attached to the endpoint.

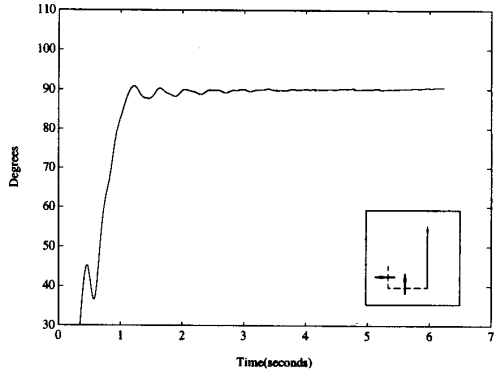

Fig. 15. Endpoint position for counter-relative slew for coupled control.

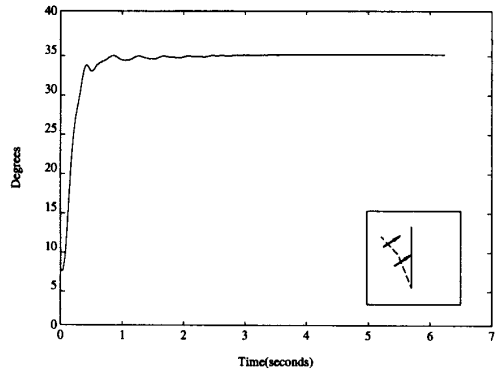

Fig. 16. Endpoint position for small slews using coupled control.

IV. Supervisory Control

The experiments using direct fuzzy control show a considerable improvement over the no-control case (Fig. 2), but are not the best possible. The uncoupled direct fuzzy controller has a fast rise time but has the drawback of having a large overshoot and oscillations near its setpoint. Coupling the two controllers via the endpoint acceleration signal reduces the overshoot and oscillation problems considerably, but makes the overall response slower due to the reduction of speed of the elbow link while the shoulder link is moving fast. This reduction of speed of the elbow link was necessary to prevent the oscillations of the elbow link endpoint near the setpoint, caused by the inertia of the links. We can overcome this problem if we are able to make a smooth transition in the speed of the shoulder link. This can be achieved by using a higher level of control for monitoring and adjusting the direct fuzzy controller. Here we will use an "expert controller" [18], [29], [19], shown in Fig. 18, which monitors the position error input $e_1(t)$ to the shoulder-motor controller and changes the fuzzy sets and the rule-base of the shoulder-motor controller. As was seen in the response for the coupled direct fuzzy controller (Fig. 14) the main cause for the hump appearing at about 0.9 seconds in the plot is the sudden change in speed of the shoulder link. The elbow link is coupled to the shoulder link using the endpoint acceleration from the shoulder link and its speed is varied depending on the oscillation of the shoulder link. To eliminate

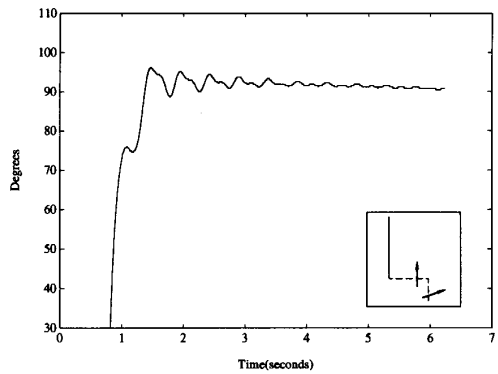

Fig. 17. Endpoint position for coupled controller design with payload.

the hump we use the expert controller to vary the speed of the shoulder link gradually so as to avoid exciting oscillatory modes which result in excessive endpoint vibrations.

The rule-base for the expert controller consists of two single-input, multiple-output rules

IF $|e_1(t)| \geq 20$ degrees **THEN** use Rule-Base 1 (Fig. 19) **AND** use expanded universes of discourse

IF $|e_1(t)| < 20$ degrees **THEN** use Rule-Base 2 (Fig. 20) **AND** use compressed universes of discourse.

The expert controller expands or compresses the universes of discourse by simply changing the normalizing gains (explained in the next subsection). When the universe of discourse is expanded, a "coarse control" is achieved, and when it is compressed, a "fine control" is achieved (this characteristic is similar to that investigated in [30]). The form of the premises of the rules of the supervisor guarantees that one (and only one) of them will always be enabled and fired at each time step. Since the control objectives can be achieved using only these two rules and only one rule will be enabled at each time step, there is no need for the use of complex inference strategies in the expert controller [19], [29].

A. Rule-Base Construction

The membership functions and the rule-base for the elbow-link controller were kept the same as in Fig. 12. In addition to the rule-base in Fig. 19, another rule-base was added for the shoulder-motor controller. The expert controller, therefore, switches between these two rule-bases for the shoulder link, for "coarse control" and "fine control." The membership functions for the coarse controller are similar to those used in the coupled direct fuzzy controller case (see Fig. 4), where the universe of discourse is [-250, +250] degrees for the position error, [-2, +2] for the endpoint acceleration, and [-1.5, +1.5] volts for the output voltage. The fine controller uses the same shape for the membership functions as shown in Fig. 4, except that the universes of discourse for the inputs and the outputs are compressed. The universe of discourse for the position error is [-25, +25] degrees, and the universe of discourse for the endpoint acceleration is [-2, +2] g. The output universe of discourse is [-0.15, +0.15] volts. Notice that while going from the coarse to the fine control, the widths of the universes of

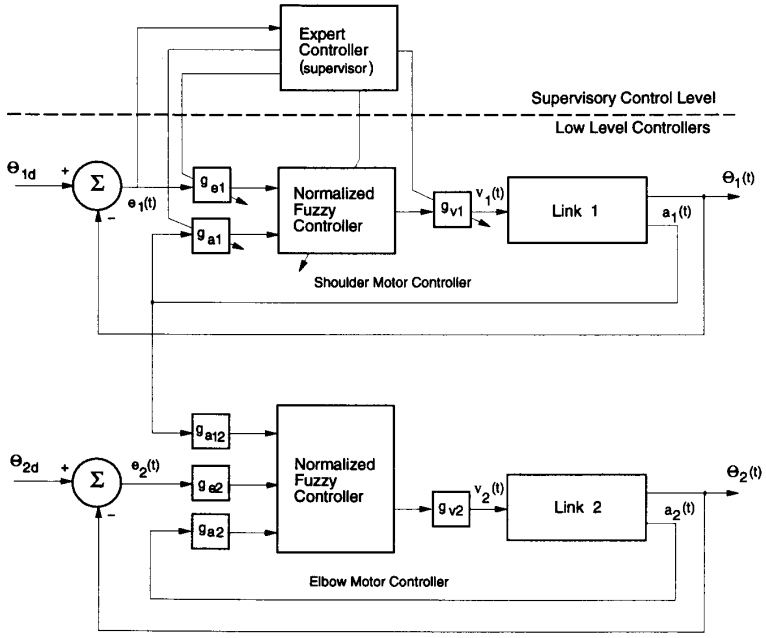

Fig. 18. Fuzzy control system with a supervisory level.

discourse for the position error and the output of the shoulder-link controller have been reduced by a factor of 10, while the width of the universe of discourse for the endpoint acceleration is reduced by a factor of two. This choice was made after several experiments, where it was found that when the width of the universe of discourse for the acceleration was reduced by a large factor the controller became too sensitive near the setpoint.

Figs. 19 and 20 show the rule-bases used for the coarse and fine control, respectively. Notice in row $j = 0$ for the rule-base for fine control, there are extra zeros as before to reduce the sensitivity of the controller to a noisy acceleration signal. The rule-base for coarse control does not have these zeros as the offset voltage from the accelerometers is of no consequence as long as the controller is operating in this region. Also notice that while the patterns in the bodies of the tables shown in Figs. 19 and 20 are similar, there are differences included to reflect the best way to control the robot. Notice that the center values in the fine control rule-base change more rapidly as we move away from the center of the rule-base as compared to the coarse control rule-base. This causes a bigger change in the output of the controller for smaller changes in the input, resulting in a better control over shaft speed of the motor, preventing it from overshooting its setpoint and at the same time causing gradual braking of the motor speed. Finally, we note that the fine control rule-base was selected so that the output is not changed too much when the rule-bases are switched, promoting a smooth transition between the rule-bases. The number of rules used by the supervisory control algorithm is 121 for the coarse controller, plus 121 for the fine controller, plus 343 for the elbow controller, plus 2 for the expert controller, resulting in a total of 587 rules. As either

V_1^n	A_1^k										
	-5	-4	-3	-2	-1	0	+1	+2	+3	+4	+5
-5	-5	-5	-5	-4	-4	-3	-3	-2	-2	-1	0
-4	-5	-5	-4	-4	-3	-3	-2	-2	-1	0	+1
-3	-5	-4	-4	-3	-3	-2	-2	-1	0	+1	+2
-2	-4	-4	-3	-3	-2	-2	-1	0	+1	+2	+2
-1	-4	-3	-3	-2	-2	-1	0	+1	+2	+2	+3
0	-3	-3	-2	-2	-1	0	+1	+2	+2	+3	+3
+1	-3	-2	-2	-1	0	+1	+2	+2	+3	+3	+4
+2	-2	-2	-1	0	+1	+2	+2	+3	+3	+4	+4
+3	-2	-1	0	+1	+2	+2	+3	+3	+4	+4	+5
+4	-1	0	+1	+2	+2	+3	+3	+4	+4	+5	+5
+5	0	+1	+2	+2	+3	+3	+4	+4	+5	+5	+5

Fig. 19. Rule-base for coarse control.

the coarse controller or the fine controller is active at any time, effectively the number of rules used is 587 - 121 = 466 rules (which is similar to what was used for the coupled direct fuzzy controller).

B. Results

Experimental results obtained using this supervisory scheme are shown in Fig. 21. The requested slew is 90 degrees for both links as shown in the inset. The response is relatively fast with very little overshoot. Comparing this response to the response obtained for the coupled direct fuzzy controller (Fig. 14) we can see that the response from the supervisory controller has a much smaller settling time and the hump in the initial portion of the graph is almost eliminated.

Fig. 22 shows the response of the robot to a counter-relative slew. The initial hump seen in the plot appears purely due to the geometry of the slew commanded and the camera position.

V_1^m \ A_1^k	-5	-4	-3	-2	-1	0	+1	+2	+3	+4	+5
-5	-5	-5	-5	-5	-4	-4	-3	-3	-2	-1	0
-4	-5	-5	-5	-4	-4	-3	-3	-2	-1	0	+1
-3	-5	-5	-4	-4	-3	-3	-2	-1	0	+1	+2
-2	-5	-4	-4	-3	-3	-2	-1	0	+1	+2	+3
-1	-4	-4	-3	-3	-2	-1	0	+1	+2	+3	+3
0	-4	-3	-2	-1	0	0	0	+1	+2	+3	+4
+1	-3	-3	-2	-1	0	+1	+2	+3	+3	+4	+4
+2	-3	-2	-1	0	+1	+2	+3	+3	+4	+4	+5
+3	-2	-1	0	+1	+2	+3	+3	+4	+4	+5	+5
+4	-1	0	+1	+2	+3	+3	+4	+4	+5	+5	+5
+5	0	+1	+2	+3	+3	+4	+4	+5	+5	+5	+5

E_1^j

Fig. 20. Rule-base for fine control.

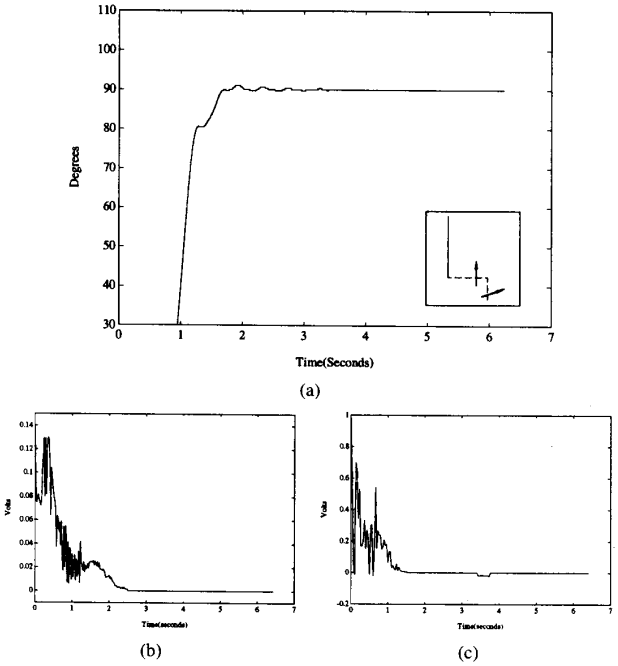

Fig. 21. (a) Endpoint position for supervisory control, (b) shoulder link input voltage v_1, (c) elbow link input voltage v_2.

The response shows an improvement over the direct fuzzy controller schemes (Figs. 17, 24) in terms of speed, overshoot, and overall settling time. The speed of the endpoint in the initial portion of the slew is more uniform as compared to the direct fuzzy control schemes and the transition in speed is smooth which prevents any overshoot in the response. This is made possible by the fine control available near the setpoint.

Fig. 23 shows the response of the robot endpoint to small commanded slews, 20 degrees for each link. The entire slew is in the visual range of the camera as can be seen from the plot. This response is comparable to the response achieved using direct fuzzy control techniques (Figs. 9 and 16).

Fig. 24 shows the response of the robot with a 30–gram payload on the endpoint. The commanded slew is 90 degrees for both the links, shown in the inset. The response is significantly improved as compared to the response from the direct

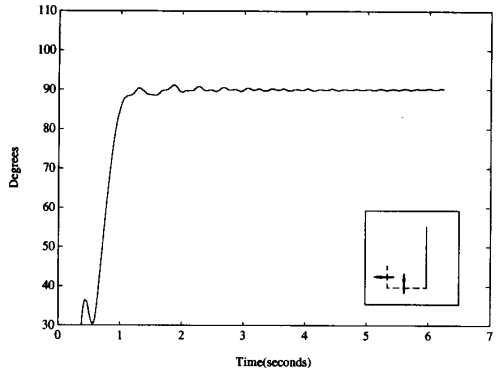

Fig. 22. Endpoint position for counter-relative slew using supervisory control.

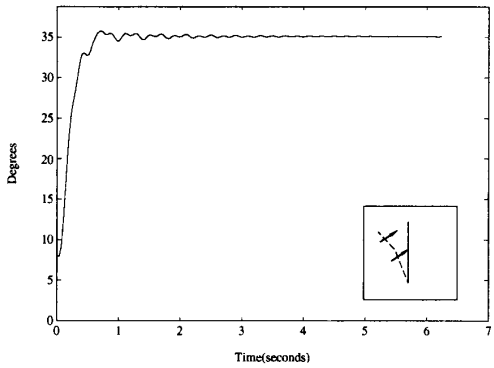

Fig. 23. Endpoint position for supervisory controller for small slew.

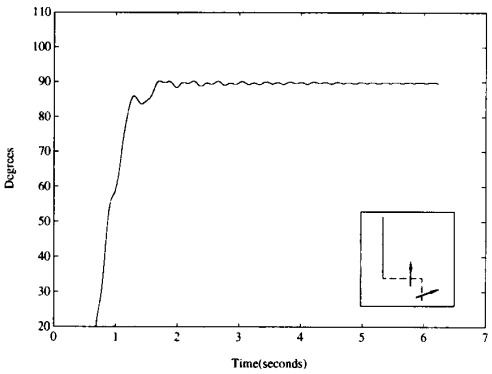

Fig. 24. Endpoint position for supervisory controller design with payload.

fuzzy control schemes (Figs. 10, 17). The oscillations in the endpoint due to the added inertia, visible in the direct fuzzy control case (Figs. 10, 17) are eliminated here.

From the results obtained for the direct fuzzy control techniques and the supervisory control technique we see that the results from the latter are consistently superior in all the cases tested. The supervisor gave better results in the case of large, counter-relative, and loaded tip slews, and was comparable to the results obtained from the direct fuzzy

controller in the case of small slews. The major difference in the implementation of the supervisory controller and the direct fuzzy controllers is the addition of the expert controller, and the additional rule-base for the shoulder-link controller. This addition does increase the complexity of the control algorithm, but not to a large extent (recall that we used 464 rules for the coupled controller and only 466 for the supervisory controller with an extra 121 for the second shoulder controller). The loop execution time increased very little, and the same sampling time (15 ms) as in the direct fuzzy control case was used. The supervisory control does use extra memory as compared to the direct fuzzy algorithms since the second rule-base (with 121 rules) for the shoulder controller had to be stored, however, in implementation, the supervisor simply has to select one rule-base or the other.

V. Conclusion

We have shown how intuitive knowledge about how to control a two-link flexible robot can be loaded into a rule-based controller to achieve endpoint position control. In particular, we investigated the performance of an uncoupled and coupled direct fuzzy controller. Moreover, we developed a hierarchical rule-based controller with an expert controller at the upper level and fuzzy controllers at the lower level. Our experimental results illustrated that for various slews and payload conditions the rule-based supervisory controller was able to achieve very good performance.

An obvious question which arises relative to this work is what performance levels have been achieved for other techniques attempted on this and similar systems. In this ongoing effort, a long and progressive history of numerous control techniques have been reported on in the open literature. These include simple linear controllers with acceleration feedback (see, e.g., [1]), nonlinear inversion techniques (feedback linearization [8]), system identification and adaptation [5], [9], [10]–[12], [15], [16], and the command input shaping techniques [3], [5], which have shown the most success prior to the supervisory approach investigated in this paper. While the rule-based supervisory control approach does in fact compare favorably to the command input shaping techniques (see the results in Section IV and compare to the results in [3]), the supervisory controller is slightly more complex to implement (both in memory and computation time requirements). A thorough comparative analysis between previous results and those reported herein would certainly be enlightening, but space limitations do not allow us to expound on the previous work. In terms of the performance objectives for this system (speed of response, minimal residual vibrations/overshoot, and smoothness of response), however, the results of the current paper are superior to all predecessors. The reader may also find it interesting that the well-known proportional-integral-derivative (PID) controller was also implemented for the flexible robot of this study. After extensive tuning of the PID gains we found that the fuzzy controllers performed much better. This was attributed to the fact that: i) the direct (coupled and uncoupled) fuzzy controllers are nonlinear controllers where due to the nonuniformity of the rule-base there is a lower gain for small signals (to avoid amplification of disturbances) and a higher gain for larger signals (to quickly drive the system to the appropriate position), and ii) the rule-based supervisory controller is an adaptive scheme that adds additional nonlinearities to achieve more effective vibration damping (e.g., the fine and coarse controls described in Section V). On the other hand, a complete comparison of the rule-based approaches to PID controllers is futile since the rule-based techniques are significantly more complex. For a more equitable comparison, consider the overview of related work above and in the introduction. Overall, we see that the rule-based approaches investigated in this paper provide an attractive alternative to conventional control approaches. This is perhaps, not too surprising since we had the benefit of many years of experience in developing and implementing conventional controllers that provided the necessary insight to be able to construct the rule-bases for the fuzzy controllers (particularly for the supervisory controller).

While we have shown that the direct fuzzy controller and rule-based supervisory controller can effectively control the two-link flexible manipulator, it is important to note that there is a need for:

i) investigations into the theoretical foundations of fuzzy control approaches and the rule-based supervisory control approaches (e.g., stability and reachability analysis),
ii) development of a more systematic methodology for constructing direct and supervisory rule-based controllers, and
iii) a more detailed comparative analysis between general rule-based supervisory control and conventional linear, optimal, adaptive, and gain scheduling approaches.

Finally, it is important to note that since the direct and the supervisory rule-based controllers were designed specifically for the experimental setup in our laboratory, it is likely that they would fail to achieve endpoint position control for other robots or plants. We emphasize, however, that the contents of this paper not only contain experimental results for the flexible robot but also illustrate a very general heuristic approach to the construction of nonlinear controllers for complex dynamical systems.

Acknowledgment

The authors would like to thank the anonymous reviewers for their helpful comments.

References

[1] S. Yurkovich, "Flexibility effects on performance and control," in *Robotic Control*, M. W. Spong, F. L. Lewis, and C. T. Abdallah, Eds. New York: IEEE Press, 1992.
[2] ——, "Motion and vibration control using command shaping methods," in *Proc. Amer. Contr. Conf.*, June 2–4 1993, San Francisco, CA, pp. 2690–2720.
[3] K. L. Hillsley and S. Yurkovich, "Vibration control of a two link flexible robot arm," *Dynam. Contr.*, vol. 3, pp. 261–280, July 1993.
[4] D. P. Magee and W. J. Book, "Eliminating multiple modes of vibration in a flexible manipulator," in *Proc. IEEE Int. Conf. Robotics Automation*, Atlanta, GA, vol. 2, , May 2–6, 1993, pp. 474–479.
[5] A. Tzes and S. Yurkovich, "An adaptive input shaping control scheme for vibration supression in slewing flexible structures," *IEEE Trans. Contr. Syst. Tech.*, vol. 1, no. 2, pp. 114–121, June 1993.
[6] S. Panzieri and G. Ulivi, "Design and implementation of a state observer for a flexible robot," in *Proc. IEEE Int. Conf. Robotics Automation*, Atlanta, GA, vol. 3, May 2–6, 1993, pp. 204–209.

[7] L. J. Alder and S. M. Rock, "Adaptive control of a flexible-link robotic manipulator with unknown payload dynamics," in *Proc. Amer. Contr. Conf.*, San Francisco, CA, June 2–4 1993, pp. 2088–2092.
[8] E. García-Benitez, J. Watkins, and S. Yurkovich, "Nonlinear control with acceleration feedback for a two-link flexible robot," *IFAC Contr. Eng. Practice*, vol. 1, no. 6, pp. 987–989, 1993.
[9] A. P. Tzes and S. Yurkovich, "Application and comparison of on-line identification methods for flexible manipulator control," *Int. J. Robotics Res.*, vol. 10, no. 5, pp. 515–527, Oct. 1991.
[10] S. Yurkovich, F. E. Pacheco, and A. P. Tzes, "On-line frequency domain information for control of a flexible-link robot with varying payload," *IEEE Trans. Automat. Contr.*, vol. 34, pp. 1300–1304, Dec. 1989.
[11] S. Yurkovich and F. E. Pacheco, "On controller turning for a flexible-link manipulator with varying payload," *J. Robotic Syst.*, vol. 6, pp. 233–254, June 1989.
[12] S. Yurkovich, A. P. Tzes, and K. L. Hillsley, "Identification and control for a manipulator with two flexible links," in *Proc. IEEE Conf. Decis. Contr.*, vol. 6, Honolulu, Hawaii, Dec. 1990, pp. 1995–2000.
[13] E. Kubica and D. Wang, "A fuzzy control strategy for a flexible link robot," in *Proc. IEEE Int. Conf. Robotics Automation*, Atlanta, GA, vol. 2, May 2–6, 1993, pp. 236–241.
[14] V. G. Moudgal, W. A. Kwong, K. M. Passino, and S. Yurkovich, "Fuzzy learning control for a flexible-link robot," in *Proc. Amer. Contr. Conf.*, Baltimore, MD, June 1994, pp. 563–567.
[15] E. García-Benitez, S. Yurkovich, and K. Passino, "A fuzzy supervisor for flexible manipulator control," in *Proc. 1991 IEEE Int. Symp. Intel. Contr.*, Arlington, VA, Aug. 1991, pp. 37–42.
[16] ——, "Rule-based supervisory control of a two-link flexible manipulator," *J. Intell. Robotic Syst.*, vol. 7, pp. 195–213, 1993.
[17] V. G. Moudgal, K. M. Passino, and S. Yurkovich, "Expert supervisory control for a two-link flexible robot," in *Proc. IEEE Int. Conf. on Robotics Automation*, San Diego, CA, May 8–13, 1994, pp. 3296–3301.
[18] K. J. Åström, J. Anton, and K. E. Arzen, "Expert control," *Automatica*, vol. 22, no. 3, pp. 277–286, 1986.
[19] P. J. Antasaklis and K. M. Passino, Eds., *An Introduction to Intelligent and Autonomous Control*. Norwell, MA: Kluwer, 1993.
[20] H. van nauta Lemke and W. De-zhao, "Fuzzy PID supervisor," in *Proc. 24th Conf. Decis. Contr.*, Ft. Lauderdale, FL, Dec. 1985, pp. 602–608.
[21] A. Ollero and A. Garcia-Gerezo, "Direct digital control, auto-tuning and supervision using fuzzy logic," *Fuzzy Sets Syst.*, pp. 135–153, 1989.
[22] C. W. DeSilva, "An analytical framework for knowledge-based tuning of servo controllers," *Eng. App. Art. Intell.*, vol. 4, no. 3, pp. 177–189, 1991.
[23] S. Tzafestas and N. Papanikolopoulos, "Incremental fuzzy expert PID control," *IEE Trans. Ind. Electron.*, vol. 37, pp. 365–371, Oct. 1990.
[24] J. R. Layne and K. M. Passino, "Fuzzy model reference learning control," in *Proc. IEEE Conf. Contr. App.*, Dayton, OH, Sept. 1992, pp. 686–691.
[25] J. R. Layne, K. M. Passino, and S. Yurkovich, "Fuzzy learning control for anti-skid braking systems," *IEEE Trans. Contr. Syst. Tech.*, vol. 1, no. 2, pp. 122–129, June 1993.
[26] J. R. Layne and K. M. Passino, "Fuzzy learning control for cargo ship steering," *IEEE Contr. Syst.*, vol. 13, pp. 23–24, Dec. 1993.
[27] V. G. Moudgal, "Direct, supervisory and adaptive fuzzy control of a two-link flexible manipulator," Master's thesis, Dept. of Elec. Eng., Ohio State Univ., Sept. 1993.
[28] C. Lee, "Fuzzy logic in control systems: Fuzzy logic controller–Part I," *IEEE Trans. Syst., Man., Cybern.*, vol. 20, pp. 404–418, Mar./Apr. 1990.
[29] K. M. Passino and A. Lunardhi, "Stability analysis of expert control systems," in *Proc. IEEE Conf. Decis. Contr.*, San Antonio, TX, Dec. 1993, pp. 765–770.
[30] Y. F. Li and C. C. Lau, "Development of fuzzy algorithms for servo systems," *IEEE Contr. Syst. Mag.*, pp. 65–72, April 1989.

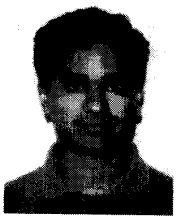

Vivek G. Moudgal received the M.S. degree in electrical engineering from The Ohio State University in 1993 and the B.E. degree in instrumentation engineering from the College of Engineering, Poona, India, in 1990.

He worked as a Project Engineer at Alfa Laval, Ltd. designing, setting up and commissioning control systems in the food and chemical industry. He is currently employed by dSPACE, Inc., Southfield, MI as an Application Engineer and is using DSP's for real time simulation and control applications.

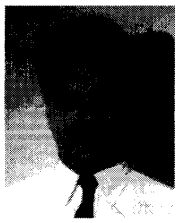

Kevin M. Passino (S'79–M'90) received the B.S.E.E. from Tri-State University, Angola, IN, in 1983 and the M.S. and Ph.D degrees in electrical engineering from the University of Notre Dame, Notre Dame, IN, in 1989.

He has worked in the control systems group at Magnavox Electronic Systems Co., Ft. Wayne, IN, on research in missile control and at McDonnell Aircraft Co., St. Louis, MO, on research in flight control. He spent a year at Notre Dame as a Visiting Assistant Professor and is currently an Assistant Professor in the Department of Electrical Engineering at Ohio State University. His research interests include intelligent and autonomous control techniques, nonlinear analysis of intelligent control systems, failure detection and identification systems, and scheduling and stability analysis of flexible manufacturing systems.

Dr. Passino is an Associate Editor for the IEEE TRANSACTIONS ON AUTOMATIC CONTROL. He served as the Guest Editor for the 1993 IEEE CONTROL SYSTEMS MAGAZINE Special Issue on Intelligent Control and is currently a Guest Editor for a special track of papers on Intelligent Control for IEEE EXPERT MAGAZINE. He is also on the Editorial Board of the *International Journal for Engineering Applications of Artificial Intelligence*. He is the Publicity Co-Chair for the IEEE Conference on Decision and Control in Japan in 1996 and was a Program Chairman for the 8th IEEE International Symposium on Intelligent Control, 1993. He is serving as the Finance Chair for the 9th IEEE International Symposium on Intelligent Control. He is co-editor (with P.J. Antsaklis) of *An Introduction to Intelligent and Autonomous Control* (Kluwer Academic, 1993). He is a member of the IEEE Control Systems Society Board of Governors. He also serves as the IEEE Control Systems Society Liaison to the IEEE Press and has served in the past as the Chairman of Student Activities for the IEEE Control Systems Society.

Stephen Yurkovich (S'79–M'82–SM'92) received the B.S. degree in engineering science from Rockhurst College in Kansas City, MO, in 1978 and the M.S. and Ph.D. degrees in electrical engineering form the University of Notre Dame in 1981 and 1984, respectively.

He held teaching and postdoctoral research positions at Notre Dame in 1984, and a Visiting Associate Professor position there in 1992. In 1984, he moved to the Department of Electrical Engineering at The Ohio State University, where he is currently Associate Professor.

Dr. Yurkovich's research, published in more than 100 technical journal articles and conference papers, includes work in the areas of system identification and parameter set estimation for control, and fuzzy logic for control, in application areas including flexible mechanical structures, intelligent vehicle highway systems, and automotive systems. He teaches a variety of undergraduate and graduate level courses in control theory, and has authored the text *Control Systems Laboratory*. In addition to being General Chair for the 1996 Conference on Control Applications, he has held numerous positions within the IEEE Control Systems Society. He is past chairman of the Standing Committees on Student Activities and on Publications, and is an elected member of the Board of Governors, was an Executive Officer in 1993, and has been elected as Vice-President for Publications for a term beginning Jan. 1, 1995. He is a Senior Member of IEEE and is currently Editor-in-Chief of *IEEE Control Systems*.